ISSN 2277-3061

Nondestructive Approach for Determination of Steel Mechanical Properties

E. López-Martínez, Jazmín Y. Juárez-Chávez, S. Serna, B. Campillo
Facultad de Química, Universidad Nacional Autónoma de México, México
edgar0902@comunidad.unam.mx
CIICAp, Universidad Autónoma del Estado de Morelos, México
jazmin@uaem.mx
CIICAp, Universidad Autónoma del Estado de Morelos, México
aserna@uaem.mx
Facultad de Química-Instituto de Ciencias Físicas, Universidad Nacional Autónoma de México, México
bci@fis.unam.mx

ABSTRACT

It was proposed the design of an artificial neural network (ANN) to estimate the yield strength in the welding zone of HSLA experimental steels. The input parameters of the ANN were the chemical composition and hardness. The information needed to training and testing the ANN was obtained by searching the literature of the yield strength as a function of the input parameters. The design was of the type perceptron multilayer with a rule learning of backpropagation type and sigmoidal transfer function, varying the number of nodes in the hidden layer. It was determined that the design of the ANN with 11 nodes is able to estimate the yield strength of high strength low alloy steels and ultra-high strength steels according to their chemical composition and hardness.

Keywords

Artificial neural network; HSLA steel; welding; heat affected zone; hardness.

Academic Discipline And Sub-Disciplines

Mechanical and Metallurgical Engineering

SUBJECT CLASSIFICATION

Welding; Mechanical Properties

TYPE (METHOD/APPROACH)

Artificial Neural Network Application; Experimental Research

ISSN 2277-3061

INTRODUCTION

In the oil industry, the hydrocarbon exploitation in extreme and/or aggressive environments and the increased production, as well as the exploitation of increasingly heavy oils has led to components (such as pipelines) made of high strength low alloy steels (HSLA) being subjected to a level of stress increasingly close to their mechanical limits with subsequent consequences. In order to prevent this, it is necessary to increase the thickness of the components, but this would involve: 1) technological challenges for the production of heavy gauge steel with the microstructural features required; 2) increase in the cost of manufacture; 3) increase in the cost of transport of manufactured components; 4) reduction of the weldability of components (distortion, residual stresses, microstructures of low temperature, softening or hardening of the heat affected zone (HAZ)); and 5) increased risk of hydrogen induced cracking (HIC) in the base material (BM) and welding zone[1-6].

To meet the requirements of hydrocarbon exploitation, it has been developed new HSLA steels (or microalloyed steels) which have higher mechanical strength and toughness, but due to the increase of them, these steels are also more susceptible to HIC, both in the BM and the welding zone. In view of this, it becomes important to characterize the mechanical properties of the new HSLA steels for the transport of hydrocarbons in the presence of hydrogen, and in particular the behavior of the welding zone, being this zone is more susceptible to HIC. Due to the microstructural changes that are experienced in the welding zone, the welded components are an example where the mechanical properties are strongly influenced by the microstructure. It is important to point out, that in the welding of thin sections, determining the mechanical properties is not an easy task, because the thickness of the welding zone (fusion zone (FZ) and HAZ) is usually narrow. Generally, the mechanical properties of the welding are not determined, instead tensile tests are perform on samples that have welding zone and BM; if failure does not occur in the welding zone, it is said that the welding has higher mechanical properties than the BM, what is known as overmatching. To determine the actual mechanical properties of the HAZ and/or FZ, it would require that these zones have a thickness large enough to obtain samples for the tension tests. Most often this is not possible, so it has been an inclination to physical simulation in specimens with dimensions such that can be performed conventional mechanical tests. These simulations have been performed with conventional isothermal heat treatments [7, 8] or by using thermomechanical simulator [9-12]. However, the behavior is relatively different between the actual HAZ and the simulated HAZ, mainly due to the microstructure surrounding the zone, specifically in a narrow HAZ thickness surrounded by other microstructures with different mechanical properties, compared with a simulated HAZ which do not have microstructural boundaries.

In the oil industry, it has been used the instrumented indentation technique to determine, based on the analysis of load-displacement curves, stress-strain curve in pipeline welds [13-15]. The nanoindentation technique, which was originally developed to determine the hardness and reduced elastic modulus [16], also has been used to determine the mechanical properties [17-19].

Because the artificial neural networks (ANNs) have proven to be a powerful tool in predicting parameters, simulation and troubleshooting engineering applications [20-28], we decided to design an ANN to estimate the yield strength of the welding zone of two HSLA experimental steels. An ANN is a network of interconnected nodes or neurons organized in layers. The basic architecture of an ANN consists of three types of layers: input layer, output layer and none or one or more hidden layers. Each node in each layer is connected to other nodes in other layers by assigning a weight factor through a learning rule [29].

To build an ANN, firstly, a database is required which is divided in two parts, one for the training step and the other for the testing step. The training step consists of feeding the ANN with information of both, independent and dependent variables (input and output parameters respectively), and by applying a transfer function, the ANN estimate the output parameters. Through a learning algorithm, the weight factors are adjusted to minimize the square error between the actual outputs and estimate outputs. The testing step involves feeding the trained ANN only with information of the input parameters, and then the output parameters are estimated. If these last are similar to the actual ones, it is said that the ANN has been tested.

The yield strength is a function of the chemical composition and microstructure, due this, the ANN design should be a function of them. Because of this, the design becomes very complex, due to the large amount of information of the microstructural characteristics (i.e. grain size, distribution and size of precipitates, number of phases, microconstituents, etc.), that need to be considered. In order to simplify the problem, instead of feeding the ANN with the microstructural characteristics, it was decided that the hardness would be one of the input parameters since it also depends on these features. In the present work we construct a database of yield strength as a function of the chemical composition and hardness of HSLA steels and ultra-high strength steels (USS). This information was used to design an ANN, and then estimate the yield strength of the welding zone of two HSLA experimental steels.

METHODOLOGY

Experimental Procedure

Two HSLA experimental steels were used in this study. These are in the form of plates and have the same chemical composition in weight percent (0.03%C, 0.24%Si, 1.00%Mn, 0.42%Cr, 0.18%Mo, 1.35%Ni, 0.02%Nb and 0.02%Ti), but with different thermomechanical treatment, so one steel is designated as M-B steel and the other F steel. On Table 1, it can be seen their corresponding hardness and yield strength.

ISSN 2277-3061

Plates were sliced to obtain two samples with the following dimensions: large 110 mm and width 110 mm with the original thickness of the plate of 11 mm.

Autogenously welding of one pass was simulated with the process of gas tungsten arc welding (GTAW), and there was neither preheating nor post-heating. The welding parameters used are shown in Table 2. To assure a high quality of the welding, the GTAW torch was adapted to a plasma cutting device. Fig 1 shows the arrangement of the welding process.

Table 1. Hardness and yield strength of the base materials

Steel	Hardness/ HV 0.1	Yield stress/ MPa
M-B Steel	311	985
F Steel	200	788

Table 2. Parameters for welding process

Current/ A	200, DCEN
Welding velocity/ m s^{-1}	0.003
Electrode	TungstenThoriated 2%
Electrode tip shape	pointed
Electrode diameter/m	0.00318

DCEN: direct current, electrode negative

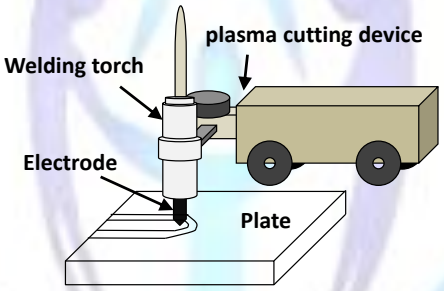

Fig 1: Adaptation of the welding torch to the plasma cutting device

After welding, cuts were made in the transverse direction of each welding to obtain samples for metallographic preparation and hardness measurement. The metallographic preparation was carried out to reveal the macrostructure, which consisted in grinding, and macro-etching with nital 6 for a period of 4 seconds. Vickers hardness measurements were made with a Shimadzu Microhardness tester model HMV-2 from the FZ to BM. The measurements were made with a force of 980.5 mN for 15s.

ANN Design

The yield strength is a function of the chemical composition and the microstructure, and this last in turn is a function of the chemical composition and thermomechanical process, so for prediction of this mechanical property, it requires a database of yield strength as a function of these two variables. Determine or find enough numerical values with these requirements, is not an easy task. To avoid this problem, the microstructural characteristics were replaced for hardness, which is a variable that depends on microstructure. Therefore, the independent variables of the ANN were the chemical composition and hardness, and the dependent variable was the yield strength. Through a literature search, a database of yield strength as a function of the chemical composition and hardness of steels was created. Information was obtained from a total of 228 HSLA and USS steels. Table 3 presents the summary of the database. In this table, it can be observed that the yield strength depends on 15 independent variables, 14 of them corresponding to the chemical composition and 1 corresponding to hardness. The database was divided in two parts; the first with 80% of the information, called training database and the second with 20% of the information called testing database. The input and output variable values of the databases were normalized using the following equation:

$$N = \frac{x_i - x_{\min}}{x_{\max} - x_{\min}} \quad (1)$$

where N is the normalized value of the x_i variable value, and x_{min} and x_{max} are the minimum and maximum values of the variable respectively. The ANN design was of the perceptron multilayer type with a back propagation learning rule and sigmoidal transfer function. A single hidden layer was used in the design of the ANN, varying the number of hidden nodes from 8 to 20, since the amount of these nodes can influence the training step, as well as in the testing step and therefor in the estimated values [30, 31]. Fig 2 shows the architecture of the ANN.

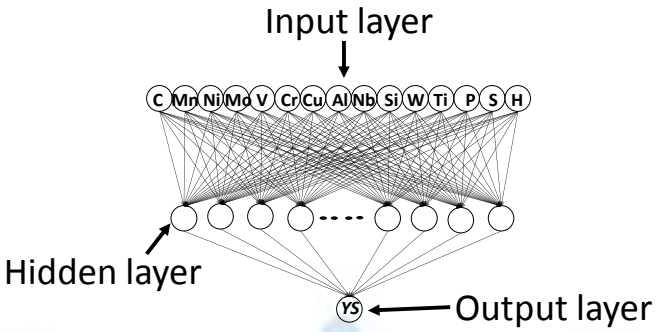

Fig 2: Architecture of the ANN. H is for hardness and YS is for yield strength

Table 3. Input and output parameters to the ANN

Parameter	Min	Max	Mean	STD
C	0	0.880	0.240	0.191
Mn	0	2.240	1.126	0.459
Ni	0	3.800	0.782	1.189
Mo	0	3.460	0.245	0.497
V	0	1.780	0.069	0.143
Cr	0	4.100	0.436	0.665
Cu	0	1.880	0.286	0.555
Al	0	0.490	0.021	0.039
Nb	0	0.860	0.044	0.147
Si	0	1.240	0.311	0.156
W	0	0.990	0.008	0.072
Ti	0	0.200	0.013	0.029
P	0	0.050	0.015	0.011
S	0	0.077	0.014	0.017
Hardness/ HV	75.80	713.0	317.6	138.1
Yield Strength/ MPa	103.0	2300.0	834.8	434.4

Once the ANN was trained and tested, it was used to estimate the yield strength in the welding zone of the M-B steel and F steel. The chemical composition of the steels and hardness of every welding zone were fed in the ANN to obtain the yield strength.

RESULTS AND ANALYSIS

The initial microstructures of M-B steel M-B and F steel, which were revealed with LePera reactive, are shown in Fig 3. It can be seen that with this reagent, we can distinguish between the different microconstituents. In the M-B steel is observed two microconstituents: martensite in white color and bainite in brown color; meanwhile, in F steel is also observed two microconstituents: ferrite in brown color and the martensite-austenite microconstituent (M-A) in white color [32]. Bainite and ferrite have similar color; this is because at lower concentrations than 1% of silicon, the colors of these

ISSN 2277-3061

microconstituents are similar [33]. With quantitative metallography, it was determined that M-B steel presents a microstructure of 30% martensite and 70% bainite, and F steel presents a microstructure of 99.2% ferrite and 0.8% M-A.

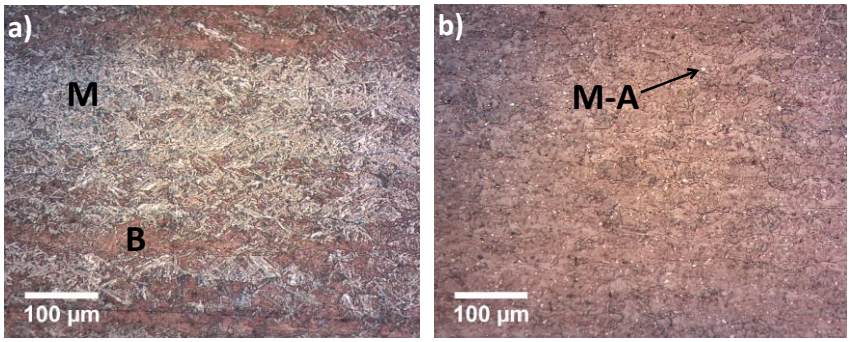

Fig 3: Microstructures of the base materials a) M-B steel, b) F steel. The withe particles in F steel are referred as M-A microconstituent

Fig 4 shows the welding produced with the GTAW process for the M-B steel, which is free of imperfections such as cracks, voids, lack of continuity, etc. Fig 5 shows the macrostructure that was developed by the effect of the heat input. It can be distinguishing the zones: FZ, HAZ and BM; and in the HAZ is distinguish the subzones: coarse grain heat affected zone (CGHAZ), which is a subzone where can be distinguished large grains; recrystallization heat affected zone (RCHAZ), where the grains are smaller and cannot be distinguish; and the intercritical heat affected zone (ICHAZ) that is between the RCHAZ and the BM. In the FZ can be seen columnar grains, which are characteristic of solidification.

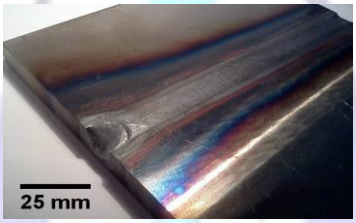

Fig 4: Welding of the M-B steel

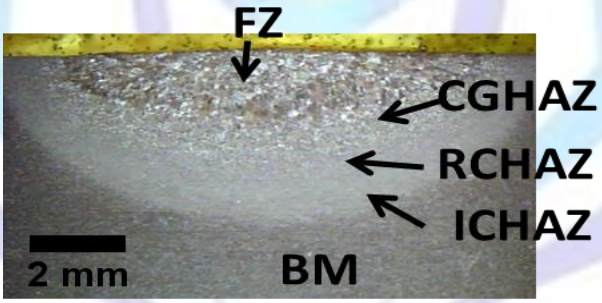

Fig 5: Macrostructure of the welding zone of the F steel

The hardness profile of the welding zone of both steels, are shown in Fig 6. It can see that the M-B steel shows a HAZ softening, but not F steel. This is due to the initial microstructure and the microstructural changes that were developed in the subzones of the HAZ, since the M-B steel has martensite in its original microstructure and for that is more susceptible to this softening [34]. In particular, in the ICHAZ, the softening is due to the tempering of martensite, because this subzone experimented a thermal cycle similar to tempering [35, 36]. This effect is not observed in the welding of the F steel, since the original microstructure is ferrite and M-A, and for that, there is not enough martensite that could be tempered.

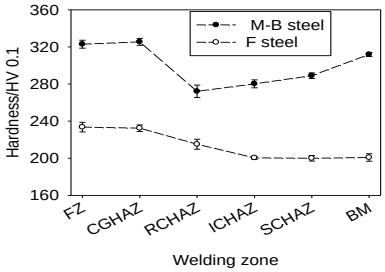

Fig 6: Hardness profiles in the welding zone

ISSN 2277-3061

All the estimated results with the ANN in the training step were compared to actual values to determine the effect of the number of nodes in the hidden layer (Fig 7). This effect is determined by obtaining the correlation coefficient from the linear regression of the data (Table 4). A correlation coefficient close to one indicates a better estimation of yield strength.

The best correlation coefficient was obtained for an ANN design with 11 nodes in the hidden layer, but regardless of the number of nodes in this layer, the ANN underestimates the yield strength for values greater than 2000 MPa.

By the difference of the estimates and actual data, the absolute error for each data pair (estimated and actual) was determined by Eq. (2)

$$Error = \left| \left(\frac{YS_e - YS_a}{YS_a} \right) * 100 \right| \quad (2)$$

where YS_e and YS_a are the estimated and actual yield strength respectively.

In Fig 8 is showed the effect of the number of nodes in the distribution of the absolute error of the estimated values in the training step. It is observed that for all de cases (8, 11, 16 and 20 nodes); the 70% of the estimated yield strengths have an absolute error of 5%. If the results with a maximum absolute error of 10% are considered, the amount of the estimated results increases up to 90% for the case of the ANN with 11 nodes. From these results, it is observed little effect on the number of nodes on the correlation coefficient and the absolute error, in which almost 100% of the estimated results have a maximum relative error of 20%. With these results, it is said that the ANN has been trained.

In Fig 9 is showed the effect of the number of nodes on the estimated yield strength in the testing step. As in the case of the training step, the effect of the number of nodes in the estimation of yield strength is determined by obtaining the correlation coefficient from the linear regression of the data (Table 4). Chemical composition and hardness, as well as the yield strength of M-B steel and F steel were included in the 20% of the database that was used in the testing step. For these steels, the lowest absolute error is obtained with 8 nodes, but the correlation coefficient is not the best as can be seen in Table 4. With 11 nodes, the absolute error between estimated and actual yield strength for M-B steel is of 7% and for F steel is of 4%, and in general, all the estimated results are the best, because is obtained the best correlation coefficient. From Fig 7, 8, 9 and Table 4 it can be seen that the best estimation of yield strengths are obtained with 11 nodes in the hidden layer of the ANN. With this, it is said that the ANN has been trained and tested.

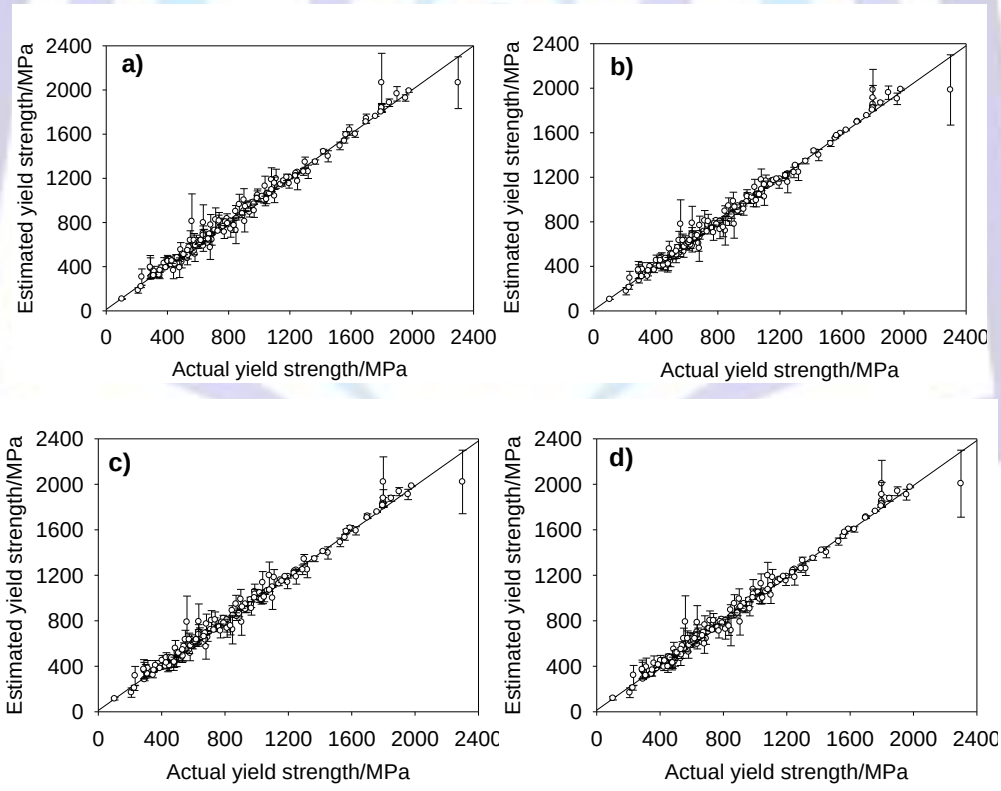

Fig 7: Effect of the number of nodes in the hidden layer on the estimation of the yield strength in the training step. a) 8 nodes, b) 11 nodes, c) 16 nodes, d) 20 nodes

ISSN 2277-3061

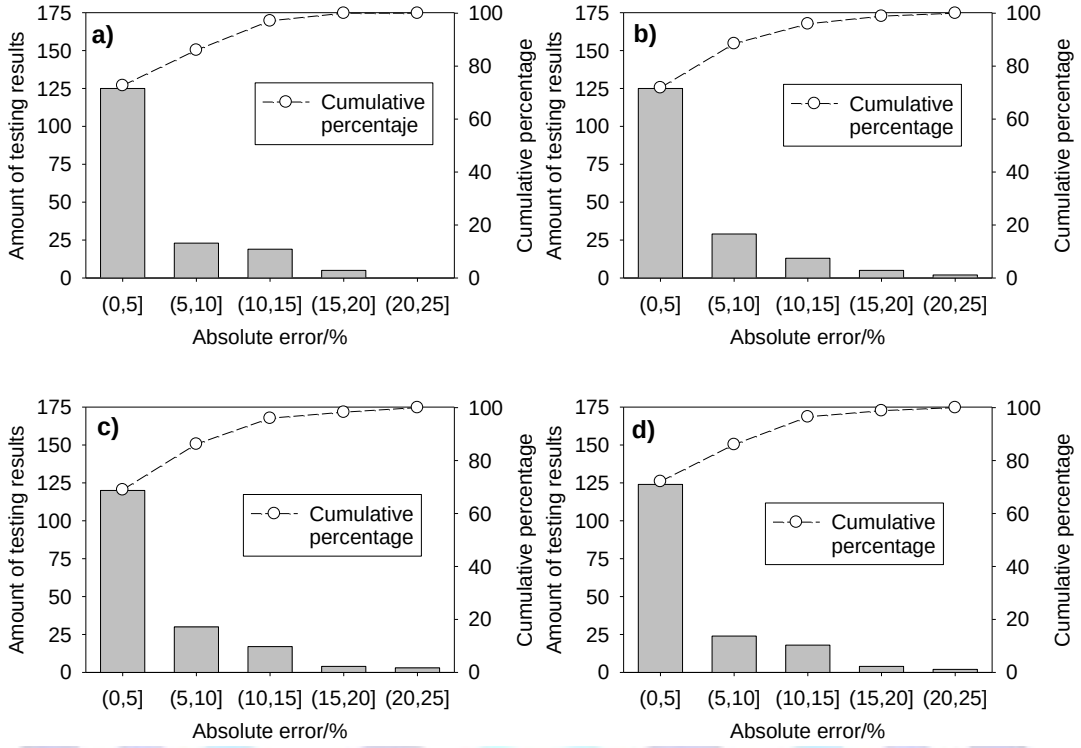

Fig 8: Distribution of the absolute error of the estimated values in the training step. a) 8 nodes, b) 11 nodes, c) 16 nodes, d) 20 nodes

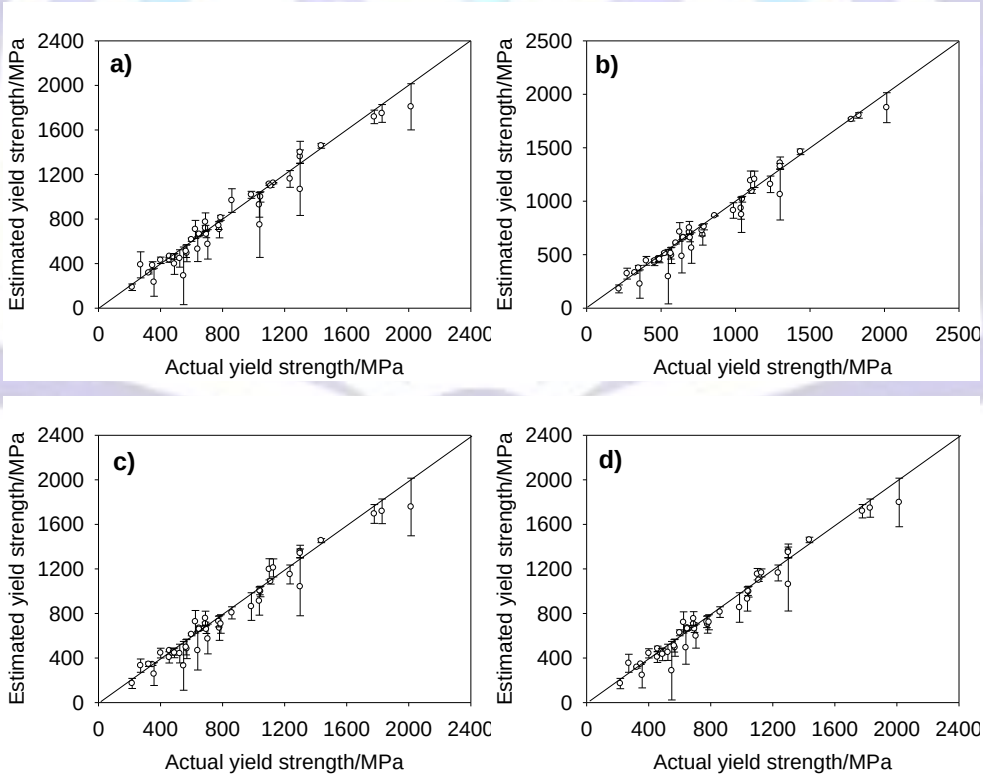

Fig 9: Effect of the number of nodes in the hidden layer on the estimation of the yield strength in the testing step. a) 8 nodes, b) 11 nodes, c) 16 nodes, d) 20 nodes.

ISSN 2277-3061

Table 4. Correlation coefficients obtained by linear regression of the ANN results in the training step and testing step

Number of nodes	R^2, training step	R^2, testing step
8	0.9849	0.9277
10	0.9835	0.9297
11	0.9852	0.9555
12	0.9852	0.9368
14	0.9847	0.9546
16	0.9849	0.9037
18	0.9837	0.9429
20	0.9851	0.9340

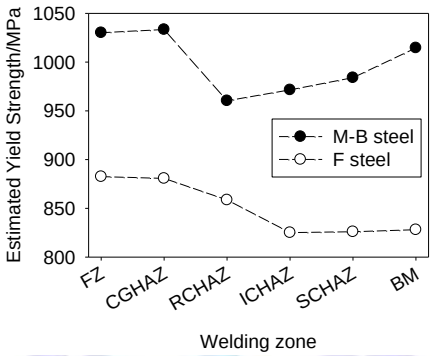

Fig 10: Estimated yield strength in the welding zone

Finally, to determine the yield strength in the welding zone of the two HSLA experimental steels, the chemical compositions and hardness profiles were fed in the trained and tested ANN. Fig 10 shows the yield strength profiles in the welding zone for both steels, which have a similar behavior to the hardness profile. M-B steel shows a higher yield strength in the CGHAZ and FZ compared with the BM; and as in the case of hardness, softening is seen in the subzones: RCHAZ, ICHAZ and subcritical heat affected zone (SCHAZ). The softening in the RCHAZ is classified as transformation softening, because the peak temperatures reached here exceeded the critical temperature A_{c1} and for that, all the original microstructure transformed to austenite in the heating cycle. In the other hand, the softening in the SCHAZ is classified as tempering softening, because the peak temperatures reached here did not exceeded the critical temperature A_{c1}, so the thermal cycle experimented in this subzone was similar to a tempering [37]. For the case of ICHAZ, transformation softening and tempering softening is presented. In F steel, the highest yield strength is presented in the FZ and CGHAZ, and softening is not observed.

CONCLUSIONS

It was trained and tested an artificial neural network to estimate the yield strength as a function of the chemical composition and hardness of HSLA and USS steels. The correlation coefficients obtained from the comparison between estimated and actual results are 0.9852 and 0.9555 for the training and testing steps respectively.

From the testing step, it was observed that the ANN is capable of predicting the yield strength of any steel that is within the limits of chemical composition and hardness of the database built.

Once trained and tested the ANN, it was used to estimate the yield strength in the welding zone of two HSLA experimental steels.

In the martensitic-bainitic steel a softening zone was observed in the RCHAZ, ICHAZ and SCHAZ which is due to phase transformation in the recrystallization subzone and tempering of martensite in the intercritical subzone, and transformation and tempering of martensite for subcritical subzone.

In the ferritic steel, a softening zone was not observed because there was not martensite in the initial microstructure that could be tempering.

ACKNOWLEDGMENTS

The authors are grateful to CONACyT grant 178777 for the financial support and for the scholarship (No 174555) to E. L.-M. Also authors are grateful to PAPIIT-UNAM grant IN118714 for the final support, and I. Puente-Lee and O. Flores from Facultad de Química-UNAM.

REFERENCES

[1] Albarran, J.L., Lopez, H.F. and Martinez, L. 1998. Crack growth in a welded microalloyed steel under sulfide stress cracking conditions. Journal of Materials Engineering and Performance. 7, (6, 1998), 777-783.

[2] Yurioka, N. and Suzuki, H. 1990. Hydrogen assisted cracking in C-Mn and low alloy steel weldments. International Materials Reviews. 35, (1, 1990), 217-249.

[3] Maday, M.-F. and Pilloni, L. 2007. The influence of hydrogen on the fatigue behaviour of base and gas tungsten arc welded Eurofer. Journal of Nuclear Materials. 367–370, Part A, (0, 2007), 516-521.

[4] Wang, S.H., Luu, W.C., Ho, K.F. and Wu, J.K. 2003. Hydrogen permeation in a submerged arc weldment of TMCP steel. Materials Chemistry and Physics. 77, (2, 2003), 447-454.

[5] Beidokhti, B., Koukabi, A.H. and Dolati, A. 2009. Effect of titanium addition on the microstructure and inclusion formation in submerged arc welded HSLA pipeline steel. Journal of Materials Processing Technology. 209, (8, 2009), 4027-4035.

[6] Mustapha, A., Charles, E.A. and Hardie, D. 2012. Evaluation of environment-assisted cracking susceptibility of a grade X100 pipeline steel. Corrosion Science. 54, (0, 2012), 5-9.

[7] Moitra, A., Parameswaran, P., Sreenivasan, P.R. and Mannan, S.L. 2002. A toughness study of the weld heat-affected zone of a 9Cr–1Mo steel. Materials Characterization. 48, (1, 2002), 55-61.

[8] Amer, A., Koo, M., Lee, K., Kim, S. and Hong, S. 2010. Effect of welding heat input on microstructure and mechanical properties of simulated HAZ in Cu containing microalloyed steel. Journal of Materials Science. 45, (5, 2010), 1248-1254.

[9] Homma, K., Miki, C. and Yang, H. 1998. Fracture toughness of cold worked and simulated heat affected structural steel. Engineering Fracture Mechanics. 59, (1, 1998), 17-28.

[10] Alvaro, A., Olden, V., Macadre, A. and Akselsen, O.M. 2014. Hydrogen embrittlement susceptibility of a weld simulated X70 heat affected zone under H2 pressure. Materials Science and Engineering: A. 597, (0, 2014), 29-36.

[11] Shi, Y. and Han, Z. 2008. Effect of weld thermal cycle on microstructure and fracture toughness of simulated heat-affected zone for a 800 MPa grade high strength low alloy steel. Journal of Materials Processing Technology. 207, (1–3, 2008), 30-39.

[12] Wang, J., Lu, S., Dong, W., Li, D. and Rong, L. 2014. Microstructural evolution and mechanical properties of heat affected zones for 9Cr2WVTa steels with different carbon contents. Materials & Design. 64, (0, 2014), 550-558.

[13] Murty, K.L., Mathew, M.D., Wang, Y., Shah, V.N. and Haggag, F.M. 1998. Nondestructive determination of tensile properties and fracture toughness of cold worked A36 steel. International Journal of Pressure Vessels and Piping. 75, (11, 1998), 831-840.

[14] Jang, J.-I., Choi, Y., Lee, J.-S., Lee, Y.-H., Kwon, D., Gao, M., et al. 2005. Application of instrumented indentation technique for enhanced fitness-for-service assessment of pipeline crack. International Journal of Fracture. 131, (1, 2005), 15-33.

[15] Schindler, H.-J. 2005. On quasi-non-destructive strength and toughness testing of elastic–plastic materials. International Journal of Solids and Structures. 42, (2, 2005), 717-725.

[16] Pharr, G.M. 1998. Measurement of mechanical properties by ultra-low load indentation. Materials Science and Engineering: A. 253, (1–2, 1998), 151-159.

[17] Dean, J., Wheeler, J.M. and Clyne, T.W. 2010. Use of quasi-static nanoindentation data to obtain stress–strain characteristics for metallic materials. Acta Materialia. 58, (10, 2010), 3613-3623.

[18] Hu, Z., Lynne, K.J., Markondapatnaikuni, S.P. and Delfanian, F. 2013. Material elastic–plastic property characterization by nanoindentation testing coupled with computer modeling. Materials Science and Engineering: A. 587, (0, 2013), 268-282.

[19] Heinrich, C., Waas, A.M. and Wineman, A.S. 2009. Determination of material properties using nanoindentation and multiple indenter tips. International Journal of Solids and Structures. 46, (2, 2009), 364-376.

[20] Dobrzański, L.A., Trzaska, J. and Dobrzańska-Danikiewicz, A.D. 2.09 - Use of Neural Networks and Artificial Intelligence Tools for Modeling, Characterization, and Forecasting in Material Engineering. In: Yilbas SHFBJVT, editor. *Comprehensive Materials Processing*. Elsevier; 2014. p. 161-198.

[21] Nazari, A., Milani, A.A. and Zakeri, M. 2011. Modeling ductile to brittle transition temperature of functionally graded steels by artificial neural networks. Computational Materials Science. 50, (7, 2011), 2028-2037.

[22] Guo, Z., Sha, W. and Li, D. 2004. Quantification of phase transformation kinetics of 18 wt.% Ni C250 maraging steel. Materials Science and Engineering: A. 373, (1–2, 2004), 10-20.

[23] Taghizadeh, S., Safarian, A., Jalali, S. and Salimiasl, A. 2013. Developing a model for hardness prediction in water-quenched and tempered AISI 1045 steel through an artificial neural network. Materials & Design. 51, (0, 2013), 530-535.

[24] Chen, N., Li, C. and Qin, P. 1998. KDPAG expert system applied to materials design and manufacture. Engineering Applications of Artificial Intelligence. 11, (5, 1998), 669-674.

[25] Mukherjee, M. and Singh, S.B. 2009. Artificial Neural Network: Some Applications in Physical Metallurgy of Steels. Materials and Manufacturing Processes. 24, (2, 2009), 198-208.

[26] Mukhopadhyay, A. and Iqbal, A. 2005. Prediction of Mechanical Properties of Hot Rolled, Low-Carbon Steel Strips Using Artificial Neural Network. Materials and Manufacturing Processes. 20, (5, 2005), 793-812.

[27] Derogar, A. and Djavanroodi, F. 2011. Artificial Neural Network Modeling of Forming Limit Diagram. Materials and Manufacturing Processes. 26, (11, 2011), 1415-1422.

[28] Mohanty*, I., Datta, S. and Bhattacharjee, D. 2008. Composition–Processing–Property Correlation of Cold-Rolled IF Steel Sheets Using Neural Network. Materials and Manufacturing Processes. 24, (1, 2008), 100-105.

[29] Jain, A.K., Mao, J. and Mohiuddin, K.M. 1996. Artificial Neural Networks: A Tutorial. Computer. 1996), 31-44.

[30] Tsai, C.-Y. and Lee, Y.-H. 2011. The parameters effect on performance in ANN for hand gesture recognition system. Expert Systems with Applications. 38, (7, 2011), 7980-7983.

[31] Teoh, E.J., Tan, K.C. and Xiang, C. 2006. Estimating the Number of Hidden Neurons in a Feedforward Network Using the Singular Value Decomposition. Neural Networks, IEEE Transactions on. 17, (6, 2006), 1623-1629.

[32] Yang, J.-h., Liu, Q.-y., Sun, D.-b. and Li, X.-y. 2010. Microstructure and Transformation Characteristics of Acicular Ferrite in High Niobium-Bearing Microalloyed Steel. Journal of Iron and Steel Research, International. 17, (6, 2010), 53-59.

[33] Girault, E., Jacques, P., Harlet, P., Mols, K., Van Humbeeck, J., Aernoudt, E., et al. 1998. Metallographic Methods for Revealing the Multiphase Microstructure of TRIP-Assisted Steels. Materials Characterization. 40, (2, 1998), 111-118.

[34] Li, J., Nayak, S.S., Biro, E., Panda, S.K., Goodwin, F. and Zhou, Y. 2013. Effects of weld line position and geometry on the formability of laser welded high strength low alloy and dual-phase steel blanks. Materials & Design. 52, (0, 2013), 757-766.

[35] Biro, E., McDermid, J.R., Embury, J.D. and Zhou, Y. 2010. Softening Kinetics in the Subcritical Heat-Affected Zone of Dual-Phase Steel Welds. Metallurgical and Materials Transactions A. 41, (9, 2010), 2348-2356.

[36] Baltazar Hernandez, V., Panda, S., Okita, Y. and Zhou, N. 2010. A study on heat affected zone softening in resistance spot welded dual phase steel by nanoindentation. Journal of Materials Science. 45, (6, 2010), 1638-1647.

[37] Hochhauser, F., Ernst, W., Rauch, R., Vallant, R. and Enzinger, N. 2012. Influence of the Soft Zone on The Strength of Welded Modern Hsla Steels. Welding in the World. 56, (5-6, 2012), 77-85.